Contents lists available at YXpublications

International Journal of Applied Mathematics in Control Engineering

Journal homepage: http://www.ijamce.com

# Modeling and Servo Control of Binocular Vision System Based on the Depth Sensitivity

Nuan Shao[a*], Zhiying Wu[a], Yang Song[a]

[a] *Department of Environmental Engineering, Hebei University of Environmental Engineering, Qinhuangdao, China*

ARTICLE INFO

Article history:
Received 15 June 2024
Accepted 22 August 2024
Available online 25 August 2024

Keywords:
Binocular visual model
Visual servo control
Depth information sensitivity
Visual tracking

ABSTRACT

In this paper, a pseudo-stereo visual model based on the concept of depth information sensitivity is presented, which uses binocular visual structure to obtain the image Jacobian matrix and eliminate the depth information Z. Then, consider the kinematics and dynamics characteristics of the robot, two image-based direct visual servo controllers are designed to control the movement of the manipulator. The aim of this approach is to move the robot arm in such a way that the target image can reach the desired position in static and motion states respectively. Theoretical analysis shows that the overall closed-loop system is stable. Finally, simulation and experiment results are used to demonstrate the performance of the proposed approach.



## 1. Introduction

Robot visual servo system is the organic integration of machine vision and robot control, it is a nonlinear, strong coupling of complex system. According to the feedback signal, visual servo systems can be grouped into position-based visual servo (PBVS), image-based visual servo (IBVS) and hybrid visual servo (HVS)[1-2]. Among them, IBVS has stronger robustness against the uncertainties and disturbance compare with the other two. It does not need to obtain 3D structure information of the scene or solve the homography matrix, and it is not sensitive to the camera calibration error. All things considered, this paper studies the robot system based on image visual servo system.

IBVS is based on the image features to complete the visual information feedback, the image plane error is loaded into the design of the controller as a direct control variable[3]. The mapping matrix between image feature space and robot operating space is called image Jacobian matrix, which is the key to the visual servo operation. For monocular visual servo system, the distance Z from the camera to the object (depth) can not be obtained directly. This is an urgent problem in solving image Jacobian matrix. A practical way is using external sensors as ultrasound, make the depth information as a fixed value substituted into the image Jacobian matrix directly[4], this method is limited to the condition of invariable depth. If the depth value change, due to the influence of computer processing speed external measuring equipment often cannot satisfy the requirement of control performance. So a large number of literatures using the approximate calculating[5] or online estimation[6-7] method to solve this problem, but due to the impact of the image information processing capabilities, parameter estimation errors tend to make the robot control task can not be achieved. In [8], a method for estimating the image Jacobian matrix is proposed based on an adaptive Kalman filter compensation algorithm. This method employs the inverse of the image Jacobian matrix in a visual servo control approach, enabling the robot's end effector to track a target object. A rapid tracking strategy for an uncalibrated visual servo system proposed in [9], this strategy utilizes the latest image information to calculate joint angles, enhancing the real-time performance of the system. In addition, to avoid performance decaying caused by measurement errors of the visual velocity, a new image-based tracking controller based on the proposal of an estimator of visual velocity was proposed in [10]. But because the presence of regression matrix, the above-mentioned controllers design are relatively complex. Due to the binocular visual system can measure the depth information of feature point, so some scholars use the layout of the cameras to avoid the estimation. Unfortunately, they are usually focus on the superposition of the monocular visual system, on the one hand, ignored the internal contact of the two cameras, on the other hand, superposition resulted in the dimension of image Jacobian matrix is too high.

In this paper, aiming at the establishment of the image Jacobian matrix problem, we present a pseudo-stereo vision model based on the depth information sensitivity. The first academic thought is the use of pseudo stereo vision variable which contains indirect correspondence relation to three dimensional information of XYZ axis. The second academic thought is using the binocular vision structure to create a new model, which does not contain depth

* Corresponding author.
E-mail addresses: selena0308@163.com (N. Shao)
Digital Object Identifiers: https://doi.org/10.62953/IJAMCE.660528

information Z and can overcome the depth visual blind spot. Our application contribution is the extension of the new binocular vision model to image-based direct visual servo control for camera-in-hand robot manipulators. In this approach, the control aim is defined in terms of the image feature error and the robot joint torques are directly computed as the control actions. Two simple image-based direct visual servo controllers for two cases are considered: position control for a fixed object and tracking control for a moving target, the effectiveness of this model is verified.

This paper is organized as follows. In Section 2, based on the concept of depth information sensitivity, a new binocular visual servo model is introduced. In Section 3, one image-based direct visual servo controller is proposed for a fixed object to position control and the dynamic stability is rigorously proved by the Lyapunov method. In Section 4, the new binocular visual model is applied for a moving target to tracking control, and the stability analysis. In Section 5, the performance of the controllers is illustrated through the simulation results. The last section presents a conclusion.

## 2. Robot Vision model

*2.1 The problem of depth information Z*

The robot visual servo systems mostly utilize the following model[11-13] (or the similar model) at the present time. Assuming that the intrinsic and extrinsic parameters of the camera are known, the time derivative of the image feature vector can be expressed as:

$$\dot{m} = J(m, Z)u \tag{1}$$

where $m = \begin{bmatrix} x \\ y \end{bmatrix}$ is the coordinate on the image plane of the feature point. $u = [T^T{}_x \quad T_y^T \quad T_z^T \quad w_x^T \quad w_y^T \quad w_z^T]^T$ is the velocity of the end-effector of the robot manipulator (including translational and rotational velocity). The image Jacobian matrix $J(m, Z)$ is given by

$$J\ (m, Z) = \begin{bmatrix} -f/Z & 0 & x/Z & \dfrac{xy}{f} & \dfrac{-(x^2+f^2)}{f} & y \\ 0 & -f/Z & y/Z & \dfrac{-(y^2+f^2)}{f} & \dfrac{-xy}{f} & -x \end{bmatrix} \tag{2}$$

Eqs. (1) and (2) are the expressions of one feature point. The biggest drawback of the model mentioned above is the unknown depth parameter *Z*. When the depth of the object is certain and known, we can control the system with trouble-free. If the depth of the object is unknown or time-varying, it is difficult to control. In some papers, the depth information is indirectly achieved through adaptive depth estimation, or simply to estimate the image Jacobian matrix [13], so the system becomes more complex. The fundamental reason of this problem is due to the monocular system can not directly measure the target's depth values.

*2.2. The problem of imaging sensitivity*

**Definition 1:** $\eta_X = \left|\dfrac{\Delta x}{\Delta Z}\right|$ will be defined as the imaging sensitivity of Deep-X axis, and $\eta_Y = \left|\dfrac{\Delta y}{\Delta Z}\right|$ will be defined as the imaging sensitivity of Deep-Y axis.

Where $\Delta x$ and $\Delta y$ are the variable quantity in x-axis and y-axis of the target point *P* in the image plane respectively, $\Delta Z$ is the variable quantity of the depth of target point *P*.

**Proposition 1:** The depth visual blind spot existing in the optical center of the monocular visual system, in where the imaging sensitivity is zero, and near the optical center can hardly provide depth information.

**Proof:** According to the monocular visual imaging principle, the relationship between image coordinate system and camera coordinate system can be expressed as follows:

$$\begin{cases} x = f\dfrac{X}{Z} \\ y = f\dfrac{Y}{Z} \end{cases} \tag{3}$$

where the focal length of the lens is $f$, *X* and *Y* denote respectively the *X-Y* coordinate of the camera coordinate system, $x$ and $y$ denote respectively the *x-y* coordinate of the image coordinate system, *Z* represents the depth information.

In order to study the relationship between depth and imaging, differentiating (3), in which Z is considered as variable, *f*, *X* and *Y* are constants:

$$\begin{cases} \dot{x} = fX\dfrac{-\dot{Z}}{Z^2} \\ \dot{y} = fY\dfrac{-\dot{Z}}{Z^2} \end{cases} \tag{4}$$

Transform (4) into incremental form, then we obtain:

$$\begin{cases} \left|-\dfrac{\Delta x}{\Delta Z}\right| = \dfrac{f|X|}{Z^2} \\ \left|-\dfrac{\Delta y}{\Delta Z}\right| = \dfrac{f|Y|}{Z^2} \end{cases} \tag{5}$$

When the target feature point locates in the optical axis (imaging center), $|X| = 0$ and $|Y| = 0$, so we can obtain that $\eta_X = 0$, $\eta_Y = 0$ from the definition of the imaging sensitivity.

Based on the concept of imaging sensitivity, it is concluded that:

In the monocular imaging system, the depth information is change. The longer distance to the image center, the more depth information can be provided, and the closer distance to the image center, the less depth information can be provided. The central point does not provide any depth information, this means that in this area, no matter what advanced algorithms we use, it could not get depth information. However, in the vicinity of the optical center—the most interesting application areas provide scarcely depth information. This is the question of depth visual blind spot.

For binocular visual servo system, only two cases of related research were found in current stage. Hiroshi KASE et al. presented a binocular visual servo control model in 1993 [14], the expression is:

$$\begin{bmatrix} \dot{x}_l \\ \dot{x}_r \\ \dot{y}_l \\ \dot{y}_r \end{bmatrix} = \begin{pmatrix} -\dfrac{s}{B} & 0 & x_l\dfrac{s}{Bf} & \dfrac{x_l y_l}{f} & \dfrac{-x_l(x_l+x_r)}{2f} - f & y_l \\ -\dfrac{s}{B} & 0 & x_r\dfrac{s}{Bf} & \dfrac{x_r y_l}{f} & \dfrac{-x_r(x_l+x_r)}{2f} - f & y_l \\ 0 & -\dfrac{s}{B} & y_l\dfrac{s}{Bf} & \dfrac{y_l^2}{f} + f & -y_l\dfrac{x_l+x_r}{2f} & -\dfrac{x_l+x_r}{2} \\ 0 & -\dfrac{s}{B} & y_l\dfrac{s}{Bf} & \dfrac{y_l^2}{f} + f & -y_l\dfrac{x_l+x_r}{2f} & -\dfrac{x_l+x_r}{2} \end{pmatrix} \begin{bmatrix} T_x \\ T_y \\ T_z \\ \omega_x \\ \omega_y \\ \omega_z \end{bmatrix} \tag{6}$$

where $s = x_l - x_r$.

This model using two cameras parallel and symmetric placement, so y-axis are the same, this structure make it possible to calculate the exact image Jacobian matrix and don't need to object modeling.

*2.3. New binocular visual servo model*

In this work, based on the concept of imaging sensitivity, make the two cameras place in parallel, in which the distance of the line connecting two lenses' optical center is *B*, the focal length of the lens is *f*, the origin *O* in the coordinate system is coincident with the origin $O_1$ of optical center of the left lens, $x_1$-$y$ and $x_2$-$y$ are the two imaging planes, due to the horizontal axis of the two imaging planes are collinear, so y-axis are the same. The imaging model is shown in Fig.1.

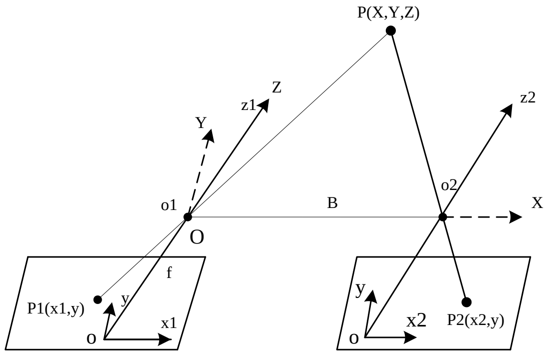


**Fig. 1.** Schematic diagram of binocular visual

The relationship between camera coordinate system and image plane coordinate system can be expressed as follows:

$$\begin{cases} X = \dfrac{x_1}{x_1 - x_2} B \\ Y = \dfrac{y}{x_1 - x_2} B \\ Z = \dfrac{fB}{x_1 - x_2} \end{cases} \tag{7}$$

If we let ${}^C P = [X, Y, Z]^T$ denote as the coordinate vector of the object point, ${}^C V = [T_X, T_Y, T_Z]^T$ denote as the linear velocity of the object point and ${}^C\Omega = [\omega_X, \omega_Y, \omega_Z]^T$ denote as the angular velocity of the object point, then the next relationship holds:

$${}^C\dot{P} = {}^C V + {}^C\Omega \times {}^C P \tag{8}$$

Take variable $\sigma = x - \theta$ as the difference between the x-axis coordinates in the left and right image planes, then the new binocular visual servo control model can be expressed as:

$$\begin{bmatrix} \dot{x}_1 \\ \dot{y} \\ \dot{\sigma} \end{bmatrix} = \begin{bmatrix} -\dfrac{\sigma}{B} & 0 & \dfrac{x_1\sigma}{fB} & \dfrac{x_1 y}{f} & -\dfrac{f^2 + x_1^2}{f} & y \\ 0 & -\dfrac{\sigma}{B} & \dfrac{y\sigma}{fB} & \dfrac{f^2 + y^2}{f} & -\dfrac{x_1 y}{f} & -x \\ 0 & 0 & \dfrac{\sigma^2}{fB} & \dfrac{y\sigma}{f} & -\dfrac{x\sigma}{f} & 0 \end{bmatrix} \cdot \begin{bmatrix} T_X \\ T_Y \\ T_Z \\ \omega_X \\ \omega_Y \\ \omega_Z \end{bmatrix} \tag{9}$$

The so-called image Jacobian matrix is defined by (10)

$$J_{image} = \begin{bmatrix} -\dfrac{\sigma}{B} & 0 & \dfrac{x_1\sigma}{fB} & \dfrac{x_1 y}{f} & -\dfrac{f^2 + x_1^2}{f} & y \\ 0 & -\dfrac{\sigma}{B} & \dfrac{y\sigma}{fB} & \dfrac{f^2 + y^2}{f} & -\dfrac{x_1 y}{f} & -x \\ 0 & 0 & \dfrac{\sigma^2}{fB} & \dfrac{y\sigma}{f} & -\dfrac{x\sigma}{f} & 0 \end{bmatrix} \tag{10}$$

where $x, y, \sigma$ are derived from the coordinate of the feature point in the image plane. The parameters of this image Jacobian matrix can be calculated in real-time. $\sigma$ is the pseudo-depth variable, for monocular or parallel binocular system, which is commonly used in parallax, here called as pseudo-depth, as long as we get the real-time coordinates and the end coordinate of this variable, then closed-loop control can be carried out, and the performance of the system is improved.

Next, we analyze the sensitivity of the depth *Z* of this model in $\sigma$ -axis. By the concept of imaging sensitivity, we can obtain:

$$\eta_{x_1} = \left| \frac{\Delta x_1}{\Delta Z} \right| \tag{11}$$

$$\eta_{x_2} = \left| \frac{\Delta x_2}{\Delta Z} \right| \tag{12}$$

Make (11) subtract (12), the imaging sensitivity in $\sigma$ -axis can be expressed as follows:

$$\begin{aligned} \eta_\sigma &= \eta_{x_1} - \eta_{x_2} \\ &= \left| \frac{\Delta x_1}{\Delta Z} \right| - \left| \frac{\Delta x_2}{\Delta Z} \right| \\ &= \frac{fB}{Z^2} \end{aligned} \tag{13}$$

We can see from (13), due to the complementary role of the left and right cameras, the imaging sensitivity in $\sigma$ -axis is a constant, overcome the poor depth information sensitivity of the existing binocular system.

## 3. Static target closed-loop control and stability analysis

We suppose the intrinsic and extrinsic parameters of the cameras are known, the feature points are always within the vision field of the cameras, by using the robot differential kinematics and the binocular visual servo model proposed in this paper we get

$$\dot{m} = J_{image} \begin{bmatrix} R_C(q) & 0 \\ 0 & R_C(q) \end{bmatrix} \begin{bmatrix} I & 0 \\ 0 & T(q) \end{bmatrix} J_A(q)\dot{q} \tag{14}$$

where $J_{image}$ is the so-called image Jacobian defined by (10), $T(q)$ is a transformation matrix that depends on the parameterization of the end-effector orientation, $J_A(q)$ is analytical Jacobian which is possible to computed the Jacobian matrix via differentiation of the direct kinematics with respect to the joint positions， $\dot{q}$ is the robot joint velocities.

Eq. (14) can be abbreviated as

$$\dot{m} = J(q, m)\dot{q} \tag{15}$$

where $J(q, m) = J_{image} \begin{bmatrix} R_C(q) & 0 \\ 0 & R_C(q) \end{bmatrix} \begin{bmatrix} I & 0 \\ 0 & T(q) \end{bmatrix} J_A(q)$ will be called the robot Jacobian matrix hereafter in this paper.

In order to verify the availability of this visual model in closed-loop control system, in the absence of friction or other disturbances, the robot dynamics can be written as

$$M(q)\ddot{q} + C(q, \dot{q})\dot{q} + G(q) = \tau \tag{16}$$

where $M(q) \in R^{n\times n}$ is a positive definite manipulator inertia matrix, $C(q, \dot{q}) \in R^{n\times 1}$ represents of centripetal and Coriolis torques, $G(q) \in R^{n\times 1}$ is gravitational torques, $\tau$ is the robot joint torques vector. In addition, the time derivative of the inertia matrix, and the centripetal and Coriolis matrix satisfy

$$\dot{x}^T \left[ \frac{1}{2}\dot{M}(q) - C(q, \dot{q}) \right] \dot{x} = 0 \tag{17}$$

This is one important property of the robot dynamics.

In this section, the control problem is to design a controller which computes the applied torques to move the robot in such a way that the actual image features reach the prescribed desired position $m_d$.

The image feature error is defined as $e = m_d - m$. Therefore, the control aim is to ensure that $\lim_{t\to\infty} e(t) = 0$.

We make the following assumptions:

**Assumption 1.** The object is static.

**Assumption 2.** There exists a robot joint configuration for which the feature error vanishes, i.e., $m_d = m(q_d)$.

**Assumption 3.** The unknown desired joint position $q_d$ is an isolated solution of $m(q) = m_d$.

In this section, we are interested in dynamic target closed-loop control and stability analysis based on the new binocular visual model.

Control scheme as shown in Fig. 2, the control law of the proposed controller is given by

$$\tau = J(q,m)^T K_p e - K_v \dot{q} + G(q) \tag{18}$$

where $J(q,m)$ is the robot Jacobian matrix, $K_p$ and $K_v$ are the symmetric positive-definite proportional and derivative matrices which are chosen by the designer.

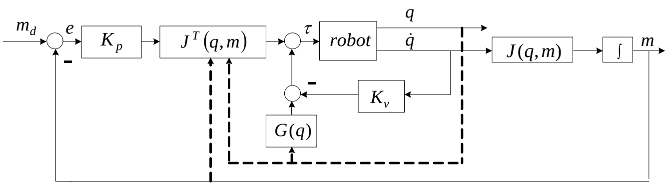


**Fig. 2.** Block diagram of visual servo control system for static objects

Substituting (18) into (16), one obtains

$$M(q)\ddot{q} + C(q,\dot{q})\dot{q} = J(q,m)^T K_p e - K_v \dot{q} \tag{19}$$

The system behavior can be written in terms of the state vector as

$$\frac{d}{dt}\begin{bmatrix} q \\ \dot{q} \end{bmatrix} = \begin{bmatrix} \dot{q} \\ M(q)^{-1}[J(q,m)^T K_p e - K_v \dot{q} - C(q,\dot{q})\dot{q}] \end{bmatrix} \tag{20}$$

In order to carry out the stability analysis, we use the Lyapunov's direct method. Thus, the following Lyapunov function candidate may be considered:

$$V = \frac{1}{2}\dot{q}^T M(q)\dot{q} + \frac{1}{2}e^T K_p e \tag{21}$$

The time derivative of (21) is given by

$$\dot{V} = \dot{q}^T M(q)\ddot{q} + \frac{1}{2}\dot{q}^T \dot{M}(q)\dot{q} - e^T K_p \dot{m}(q) \tag{22}$$

By using the closed-loop equation (15) and (19), it follows that

$$\begin{aligned} \dot{V} = {} & \dot{q}^T\left[J(q,m)^T K_p[m_d - m] - K_v\dot{q} - C(q,\dot{q})\dot{q}\right] \\ & + \frac{1}{2}\dot{q}^T\dot{M}(q)\dot{q} - [m_d - m]^T K_p J(q,m)\dot{q} \end{aligned} \tag{23}$$

After some simplifications and using (17), it is finally obtained

$$\dot{V} = -\dot{q}^T K_v \dot{q} \le 0 \tag{24}$$

The result confirms that the visual servo system is asymptotically convergent in its workspace under the control law $\tau$, i.e., $\lim_{t\to\infty} e(t) = 0$ as $\dot{q} = 0$. This means that the control aim is achieved.

## 4. Dynamic target closed-loop control and stability analysis

When the tracking target is moving, the desired joint position $q_d$ is considered as variable, so $\dot{q}_d \ne 0$. When the system reaches the desired trajectory, then we have that $e = m_d - m \to 0$, $\dot{e} = \dot{m}_d - \dot{m} \to 0$, i.e., $m = m_d$, $q = q_d$, $\dot{m} = \dot{m}_d$, $\dot{q} = \dot{q}_d$.

Define the joint position error as $e_q = q_d - q$. In this design, by using (15) we make the image feature error $e$ as

$$\dot{e} = J(q,m)\dot{e}_q \tag{25}$$

Control scheme are shown in Fig. 3. The control law is given by

$$\begin{aligned} \tau = {} & M(q)J^+(q,m)\ddot{m}_d + \left[M(q)\dot{J}^+(q,m) + C(q,\dot{q})J^+(q,m)\right. \\ & \left. + K_v J^+(q,m)\right]\dot{m}_d + J^T(q,m)K_p e - K_v\dot{q} + G(q) \end{aligned} \tag{26}$$

where $J^+(q,m)$ is pseudo inverse matrix of $J(q,m)$, $K_p$ and $K_v$ are the symmetric positive-definite proportional and derivative matrices which are chosen by the designer.

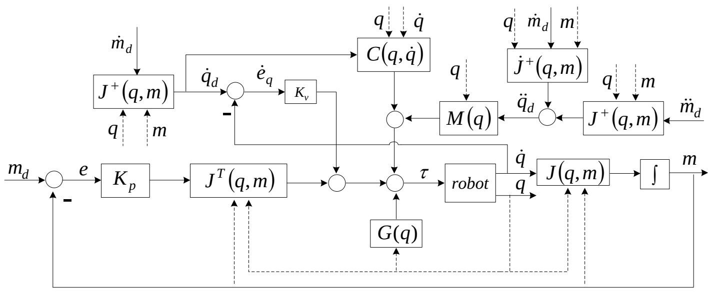


**Fig. 3.** Block diagram of visual servo control system for dynamic objects

In order to carry out the stability analysis, the Lyapunov function is given by

$$V = \frac{1}{2}\dot{e}_q^T M(q)\dot{e}_q + \frac{1}{2}e^T K_p e \tag{27}$$

The time derivative of (27) is obtained

$$\dot{V} = \dot{e}_q^{\,T} M(q)\ddot{e}_q + \frac{1}{2}\dot{e}_q^{\,T}\dot{M}(q)\dot{e}_q + e^T K_p \dot{e} \tag{28}$$

According to (26), (25), (16), (15) and the characteristics of (17), we have that

$$\begin{aligned} \dot{V} &= \left(J^+(q,m)\dot{e}\right)^T\left(M(q)\ddot{e}_q + C(q,\dot{q})\dot{e}_q - C(q,\dot{q})J^+(q,m)\dot{e}\right) + \frac{1}{2}\left(J^+(q,m)\dot{e}\right)^T\dot{M}\left(J^+(q,m)\dot{e}\right) + e^T K_p\dot{e} \\ &= \left(J^+(q,m)\dot{e}\right)^T[-J^T(q,m)K_p e - K_v\dot{e}_q] + e^T K_p \dot{e} \\ &= -\left(J^+(q,m)\dot{e}\right)^T J^T(q,m)K_p e - \left(J^+(q,m)\dot{e}\right)^T K_v\left(J^+(q,m)\dot{e}\right) + e^T K_p\dot{e} \\ &= -\dot{e}_q^{\,T} K_v \dot{e}_q \end{aligned} \tag{29}$$

Since $K_v$ is by design a positive-definite matrix, hence, $\dot{V}$ is a globally negative-semidefinite function. Therefore, $\left[q^T \quad (\dot{q}_d - \dot{q})^T\right]^T = \left[q_d^T \quad 0\right]^T$ is stable equilibrium. Invoking the LaSalle's theorem, $J^T(q,m)K_p e = 0$ as $\dot{q}_d = \dot{q}$, i.e., $\lim_{t\to\infty} e(t) = 0$. The actual image features reach the prescribed desired ones and synchronized motion with the target.

## 5. Simulation results

In this section, the performance of the proposed controllers were demonstrated by simulations. The simulations were conducted on a 2 DOF manipulator as shown in Fig. 4.

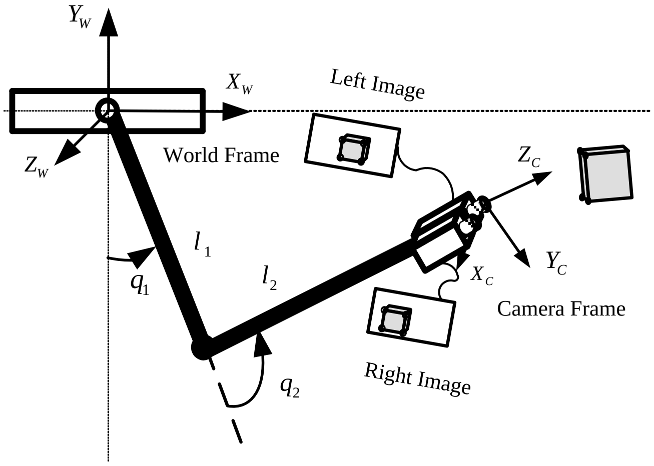


**Fig.4**. System Diagram

### 5.1. Position control for a fixed object

We use the control program as shown in Fig. 2. Take a rectangular image as the object and choose its four vertices as feature points. Their starting coordinate values are $m_{01}=[44.7;17.7;89.5]$ ; $m_{02}=[44.7;-71.7;89.5]$ ; $m_{03}=[-44.7;-71.7;89.5]$ ; $m_{04}=[-44.7;17.7;89.5]$ ; and the desired feature points are $m_{d1}=[68.4;109.6;136.8]$ ; $m_{d2}=[68.4;-27.2;136.8]$ ; $m_{d3}=[-68.4;-27.2;136.8]$; $m_{d4}=[-68.4;109.6;136.8]$. The distance of the two lenses' optical center $B$=100 mm, the initial pose of the robot manipulator $q_1(0)$=45°, $q_2(0)$=90°. The movement curve of the feature points is shown in Fig.5. Fig.6 depicts the time evolution of the image features error.

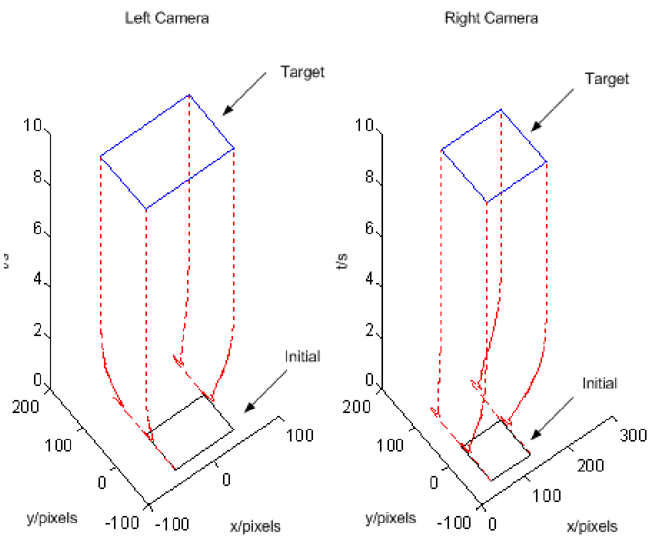


**Fig.5.** Trajectory in the 3D plane

From Fig.5 we can see that the image features arrived at the desired location and as time goes on, the depth value change along with the distance between cameras and object after a short fluctuation. From Fig.6 we can see that the error of the image features converge to zero at about five seconds, the camera reaches the desired position.

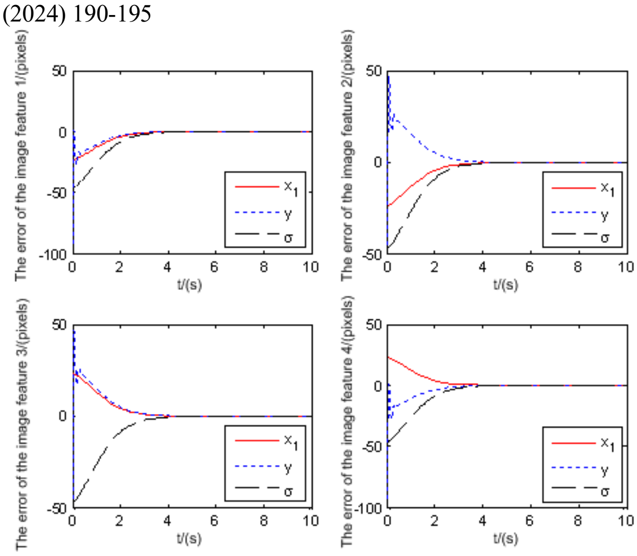


**Fig.6**. Time histories of the image features error

### 5.2. Dynamic object tracking control

In order to highlight the experimental results, still with two joint hand-eye system as an example, we use the control program as shown in Fig.3. It is considered that two point objects move within the manipulator's environment by describing a circular trajectory with bounded velocity, the desired trajectory of the manipulator's end-effector in the image plane are $m_{d1}=\begin{bmatrix}67\cos t & 127\sin(t+pi/4) & 135\cos t\end{bmatrix}^T$ , $m_{d2}=\begin{bmatrix}54\cos t & 130\sin(t+pi/4) & 110\cos t\end{bmatrix}^T$, the initial pose of the robot manipulator $\begin{bmatrix}q_{10} & q_{20}\end{bmatrix}^T=\begin{bmatrix}45^\circ & 90^\circ\end{bmatrix}^T$. Fig.7 shows the three-dimensional trajectory of the manipulator's end-effector during the tracking process, the solid lines show the tracking trajectory and the dotted lines indicate the desired trajectory. Fig.8 depicts the position error curve of the two feature points.

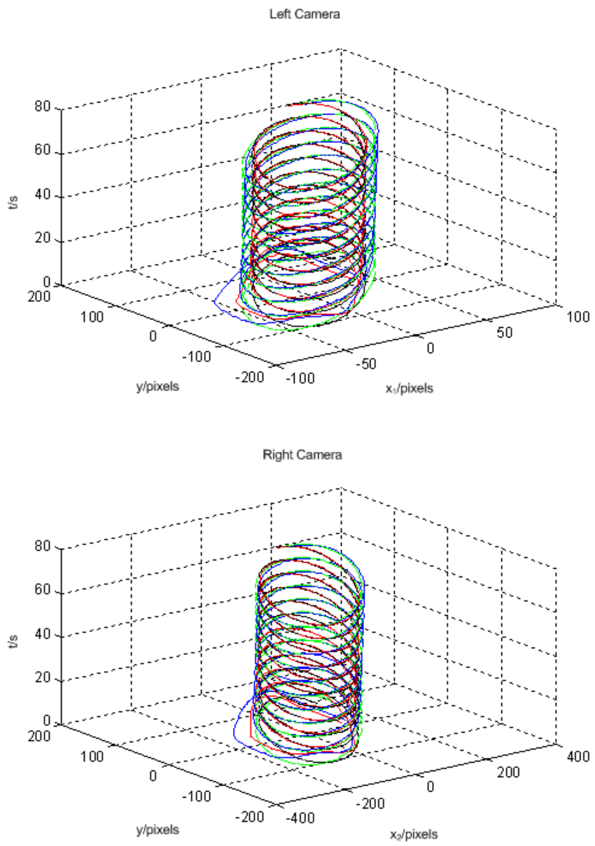


**Fig.7**. Tracking trajectory of the cameras in 3D plane

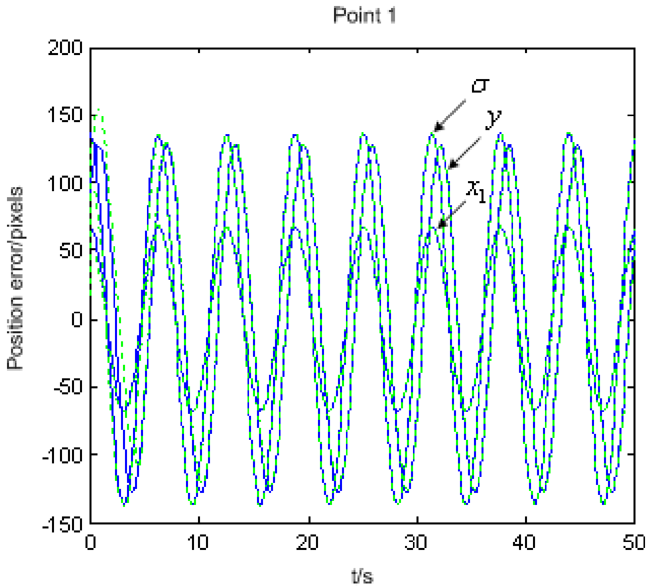


**Fig.8**. The position error curve

From the simulation results, we can see that the position errors asymptotically tend to zero, the manipulator's end-effector stable to keep up with the reference trajectory and synchronous movement with it. The effectiveness of the proposed controller is verified by the simulations.

## 6. Conclusion

According to the limitations of the existing visual model, this paper puts forward the concept of depth information sensitivity and derives a model for binocular visual servo control. This model solves two problems: poor depth information sensitivity and existence of the depth variable Z. It will make the control system more reasonable and simplified. Our application contribution is the extension of the new binocular vision model to image-based direct visual servo control for camera-in-hand robot manipulators. Two simple controllers are designed to position control for a fixed object and tracking control for a moving target. The simulation results are shown that the system established based on the new model can be able to control the end-effector of manipulator move from the initial position to the desired location and follow the target synchronous movement.

## Acknowledgements

This work was funded by Science Research Project of Hebei Education Department under Grant No. QN2022134.

## References

[1] C. Chen, Y. Y. Tian, L. Lin, et al. Obtaining world coordinate information of UAV in GNSS denied environments [J]. Sensors, 2020, 20(8): 2241.

[2] F. Janabi-Sharifi, L. F. Deng, W. J. Wilson. Comparison of basic visual servoing methods [J]. IEEE/ASME Transactions on Mechatronics, 2011, 16(5): 967-983.

[3] H. Tan. Overview of control methods for mobile robots [J]. Technology Innovation and Application, 2021, 11(20): 125-127.

[4] K. Rafael, C. Ricardo, N. Oscar, et al. Stable visual servoing of amera-in-hand robotic systems [J]. IEEE/ASME Transactions on Mechatronics, 2000, 5(1): 39-48

[5] B. Tao, Z. Gong, H. Ding. Survey on uncalibrated robot visual servoing control [J]. Chinese Journal of Theoretical and Applied Mechanics, 2016, 48(4): 767-783.

[6] X. J. Zeng, X. H. Huang, M. Wang. Vision servoing based on online estimation of image Jacobian matrix of broyden [J]. Journal of Huazhong University of Science and Technology, 2008, 36(9): 17-20.

[7] X. Lv, X. Huang. Fuzzy adaptive Kalman filtering based estimation of image Jacobian for uncalibrated visual servoing [C]. In Proc. IEEE/RSJ International Conference on Intelligent Robots and Systems, Beijing, China, 2006, 2167-2172.

[8] D. X. Sun. Research on model prediction method of robot visual [D]. Changchun University of Technology, 2018.

[9] S. J. Ma, T. Z. Tie, Y. L. Wang, et al. A fast tracking strategy for uncalibrated visual servo system [J]. Journal of Northeastern University ( Natural Science), 2020, 40(3): 355-360.

[10] H. S. Wang, Y. H. Liu, W. D. Chen. Uncalibrated visual tracking control without visual velocity [J]. IEEE Transactions on Control Systems Technology, 2010, 18(6): 1359-1370.

[11] V. Andaluz, R. Carelli, L. Salinas, et al. Visual control with adaptive dynamical compensation for 3D target tracking by mobile manipulators [J]. Mechatronics, 2012, 22(4): 491-502.

[12] B. Morales, F. Roberti, J. M. Toibero, R. Carelli. Passivity based visual servoing of mobile robots with dynamics compensation [J]. Mechatronics, 2012, 22(4): 481-490.

[13] D. I. Kosmopoulos. Robust Jacobian matrix estimation for image-based visual servoing [J]. Robotics and Computer-Integrated Manufacturing, 2011, 27(1): 82-87

[14] H. Kase, N. Maru, A. Nishikawa, et al. Visual servoing of the manipulator using the stereo vision [C]. Industrial Electronics, Control, and Instrumentation, 1993, 3: 1791- 1796.

***Nuan Shao*** An associate professor at the department of environmental engineering, Hebei university of environmental engineering, China. She received the Ph.D. degree in control science and engineering from the Yanshan university in 2015. Her research interest covers image signal processing, robot visual control and tracking control of multi-robot system.

***ZhiYing Wu*** A professor at the department of environmental engineering, Hebei university of environmental engineering, China. She received the Ph.D. degree in control science and engineering from the Dalian university of technology in 2013. Her research interest covers visual tracking control of multi-agent system.

***Yang Song*** A lecturer at the department of environmental engineering, Hebei university of environmental engineering, China. She received the M.E. degree in mechanical design and automation from the Dalian ocean university in 2009. Her research interest covers environmental protection equipment design and manufacture.